ARTICLE NO. 79-4122

Settling Times of Pressure Measurements through Capillary Tubes

Junzo Sato*
University of Tokyo, Tokyo, Japan

A settling time of pressure instrumentation connected through long, thin capillary tubes is studied theoretically and experimentally. A nonlinear partial-differential equation of heat flow type is derived under an assumption of laminar subsonic isothermal flow for pressure variations along tubes with small radius to length ratios. The equation is integrated numerically for problems with initial stepwise pressure difference assumed to be at the open end of tubes (case A) or at the junction of tubes and pressure transducers (case B); the results are compared with experiments, which show fair agreement as long as the Reynolds number is small. The pressure settling times are shown to depend heavily on the tube radius to length ratio, the tube inside volume to pressure transducer cavity volume ratio, and the absolute value of the pressure to be measured, whereas the dependence on the initial pressure difference across the tube is weak. The existence of a front of pressure variation that travels within tubes is proved and the speed of compression fronts is shown to be smaller than that of expansion ones. The approximate settling time estimation formulas appropriate for very long, thin capillary tubes are presented.

I. Introduction

WIND tunnel pressure distribution measurements on models have to rely on static pressure holes with small diameters to secure spatial resolution of distributions, particularly around the leading edge of airfoils. Also the pressure tubes must be thin in order to be installed inside of models that are required to have strength and rigidity in high dynamic pressure flows. The model inside volumes, in most cases, are insufficient to house pressure scanning devices as well as pressure transducers; therefore, the length of tubing cannot be made short. Furthermore, running times of some testing facilities[1] are very short (less than several seconds), and it is not easy to make high-accuracy pressure-distribution measurement scanning among many long, thin tubes within short intervals.

In the present paper, the following two types of pressure response time histories within pressure tubings and pressure transducers are investigated for long, thin tubes:

1) Case A: Time history of pressure variation in response to a stepwise pressure change at static pressure holes. This case estimates a time lag between idealized wind tunnel startings and establishment of steady-state outputs of pressure transducers (Fig. 1a).

2) Case B: Time history of pressure variation in response to a sudden release of valves connecting tubings and pressure transducers. This case corresponds to estimating necessary scanning time intervals to measure accurate pressures at various static holes connected with one transducer (Fig. 1b).

The case A response has been studied by a number of researchers in connection with shock tubes as well as blow-down supersonic wind tunnels.[2-4] These works, however, are mostly for moderate to short tubings, except the one made by Ducoffe,[4] who studied long, thin tubes. No systematic studies on case B have been reported yet.

Ducoffe's simple assumption of local, steady, incompressible Poiseuille flow within tubes is to be verified in this paper through more rigorous derivation of the basic equations.

II. Basic Equations for Theoretical Analysis

The pressure-measuring instrumentation is composed of a pressure hole, a capillary tube (with length L and inner radius R), a solenoid valve, and a pressure transducer coupled with a connector to the tubing (Figs. 1a and 1b). The connector and the pressure transducer comprise a cavity of volume V. The pressure $\hat{P}_0$ measured through static holes is assumed constant at all times, and the effects of flow outside the holes are neglected. Furthermore, by assuming that the heat capacity of tube walls is sufficiently large and the inner radius of tubes small, the flow within tubes is taken as a laminar axisymmetric viscous flow of an isothermal perfect gas.

The nondimensional basic equations for the flow within tubes are, therefore, an equation of continuity

$$\frac{\partial \rho}{\partial t} + \frac{\partial \rho u r}{r \partial r} + \frac{\partial \rho w}{\partial z} = 0 \tag{1}$$

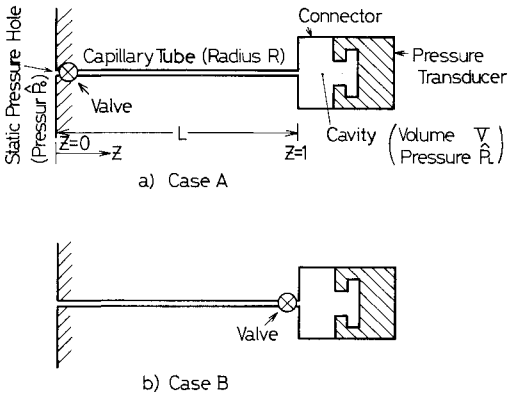

Fig. 1 Schematic illustrations of the pressure measuring systems.

Received Sept. 29, 1978; revision received April 12, 1979. Copyright © American Institute of Aeronautics and Astronautics, Inc., 1978. All rights reserved. Reprints of this article may be ordered from AIAA Special Publications, 1290 Avenue of the Americas, New York, N.Y. 10019. Order by Article No. at top of page. Member price $2.00 each, nonmember, $3.00 each. **Remittance must accompany order.**

Index categories: Nonsteady Aerodynamics; Viscous Non-boundary-Layer Flows.

*Associate Professor, Department of Aeronautics. Member AIAA.

the Navier-Stokes equations

$$\rho\frac{Du}{Dt}=-\frac{\partial P/\partial r}{\gamma M_0^2}+\frac{1}{R_e}\left\{\frac{\partial}{\partial r}\left(\frac{2\partial u}{\partial r}-\frac{2\mathrm{div}v}{3}\right)+\frac{\partial}{\partial z}\left(\frac{\partial u}{\partial z}+\frac{\partial w}{\partial r}\right)+\frac{2}{r}\left(\frac{\partial u}{\partial r}-\frac{u}{r}\right)\right\} \tag{2}$$

$$\rho\frac{Dw}{Dt}=-\frac{\partial P/\partial z}{\gamma M_0^2}+\frac{1}{R_e}\left\{\frac{\partial}{\partial z}\left(\frac{2\partial w}{\partial z}-\frac{2\mathrm{div}v}{3}\right)+\frac{1}{r}\frac{\partial}{\partial r}r\left(\frac{\partial u}{\partial r}+\frac{\partial w}{\partial r}\right)\right\} \tag{3}$$

and an equation of state for an isothermal perfect gas

$$P=\rho \tag{4}$$

where

$$\frac{D}{Dt}=\frac{\partial}{\partial t}+u\frac{\partial}{\partial r}+w\frac{\partial}{\partial z} \tag{5}$$

$$\mathrm{div}v=\frac{\partial u}{\partial r}+\frac{\partial w}{\partial z}+\frac{u}{r} \tag{6}$$

$$\epsilon=\frac{R}{L} \tag{7}$$

$$M_0=\frac{\hat{W}_0}{\sqrt{\gamma\hat{P}_0/\hat{\rho}_0}} \tag{8}$$

$$R_e=\hat{\rho}_0\frac{\hat{W}_0 L}{\mu_0} \tag{9}$$

and r is the radial and z the axial coordinate with the origin placed at the center of the static pressure hole; velocity components in the r and z directions are u and w, respectively; t is the time; ρ the density; P the pressure; and γ the ratio of specific heats. Whole variables are nondimensionalized through the pipe length L, mean axial velocity $\hat{W}_0$, pressure $\hat{P}_0$, density $\hat{\rho}_0$ of the gas outside the static hole, and the viscosity coefficient μ_0 of the gas within tubes.

The boundary conditions at $r=R/L$ are:

$$u=w=0 \tag{10}$$

III. Thin Capillary Approximation

The pressure tubes are assumed to be thin and long; therefore, two widely different length scales R and L exist. If $F(z)$ is assumed to be an arbitrary function of z, it can be written as a function of two variables Z and z^* which are of order unity in each length scale L and R, respectively:[5]

$$F(z)=G(Z,z^*) \tag{11}$$

where

$$\begin{aligned} Z&=z \qquad (z \text{ variable in scale } L)\\ z^*&=z/\epsilon \qquad (z \text{ variable in scale } R)\end{aligned} \tag{12}$$

From Eq. (11)

$$\frac{dF}{dz}=\frac{\partial G}{\partial Z}\frac{\partial Z}{\partial z}+\frac{\partial G}{\partial z^*}\frac{\partial z^*}{\partial z}=\frac{\partial G}{\partial Z}+\frac{1}{\epsilon}\frac{\partial G}{\partial z^*} \tag{13}$$

holds.

Furthermore, two variables of order unity in the radial direction

$$r^*=r/\epsilon \quad \text{and} \quad u^*=u/\epsilon \tag{14}$$

are introduced, and

$$1/R_e\sim O(\epsilon) \tag{15}$$

is assumed, which is a case of interest since both the assumptions of $R_e\sim$O(1) or $R_e\sim$O($1/\epsilon^2$) yield, in their first approximation in ϵ, trivial problems of Stokes or inviscid flow, respectively.

The time variable t can also be divided into two variables:

$$T=t \quad \text{in scale } L \quad \text{and} \quad t^*=t/\epsilon \quad \text{in scale } R \tag{16}$$

The variable t^* is important, particularly for research on turbulence or propagation of sharp discontinuities such as shock waves, but the present paper is concerned only with the relatively slow variation of pressure along tubes, thus the time variable is assumed to have order unity in scale L. This limits the applicability of the theory to laminar subsonic flow.

Now, Eqs. (11), (13), and (14) are substituted into Eqs. (1-4), and the terms of the same order in ϵ are equated to zero; i.e.,

$$\mathrm{O}(1/\epsilon): \qquad \frac{\partial\rho w}{\partial z^*}=0 \tag{17}$$

$$\frac{1}{\gamma M_0^2}\frac{\partial P}{\partial r^*}-\frac{1}{3R_e\epsilon}\frac{\partial^2 w}{\partial z^*\partial r^*}=0 \tag{18}$$

$$\rho w\frac{\partial w}{\partial z^*}+\frac{1}{\gamma M_0^2}\frac{\partial P}{\partial z^*}-\frac{1}{R_e\epsilon}\left(\frac{4}{3}\frac{\partial^2 w}{\partial z^{*2}}+\frac{\partial}{r^*\partial r^*}\frac{r^*\partial w}{\partial r^*}\right)=0 \tag{19}$$

$$\mathrm{O}(1): \qquad \frac{\partial\rho}{\partial t}+\frac{\partial\rho u^* r^*}{r^*\partial r^*}+\frac{\partial\rho w}{\partial Z}=0 \tag{20}$$

The other equations of order unity and the higher order ones are neglected in the following analysis. Moreover, a relation which states variation of density over the scale length R is negligibly small

$$\frac{\partial\rho}{\partial z^*}=0 \tag{21}$$

can be prescribed to remove the arbitrariness involved in the definition of the function G by Eq. (11); this amounts to the assumption of incompressible flow in scale R.

From Eqs. (17) and (21),

$$\frac{\partial w}{\partial z^*}=0 \quad \text{or} \quad w=w(t,r^*,Z) \tag{22}$$

and from Eqs. (18) and (22),

$$\frac{\partial P}{\partial r^*}=0 \quad \text{or} \quad P=P(t,Z,z^*) \tag{23}$$

Furthermore, Eq. (10) reduces to

$$\frac{\partial P}{\partial z^*}=\frac{\gamma M_0^2}{R_e\epsilon}\frac{\partial}{r^*\partial r^*}\frac{r^*\partial w}{\partial r^*} \tag{24}$$

which can be integrated with the aid of Eqs. (10) and (23) to give

$$w(t,r^*,Z)=-\frac{R_e\epsilon}{4\gamma M_0^2}(1-r^{*2})\frac{\partial P}{\partial z^*} \tag{25}$$

This velocity distribution is exactly the same as that of the Hagen-Poiseuille flow[6] in circular tubes.

Since incompressible flow is assumed in scale R, a new equation of state

$$\rho=\rho(\hat{T}_0) \tag{26}$$

for the isothermal incompressible gas must be substituted for Eq. (4), where $\hat{T}_0$ is the tube wall temperature.

Now, if Eq. (20) is multiplied with $2\pi r^*$ and integrated with respect to r^* from $r^*=0$ to $r^*=1$, an equation for the mean density over the tube cross section is obtained as follows;

$$\frac{\partial\bar{\rho}}{\partial t}+\frac{\partial\overline{\rho w}}{\partial Z}=0 \tag{27}$$

where

$$\bar{\rho}=\frac{1}{\pi}\int_0^1 2\pi r^*\rho\,dr^* \tag{28}$$

$$\overline{\rho w}=\frac{1}{\pi}\int_0^1 2\pi r^*\rho w\,dr^* \tag{29}$$

From Eqs. (4), (21), and (23)

$$\rho(t,Z)=\bar{\rho}(t,Z)=P(t,Z) \tag{30}$$

holds in scale L. Substitution of Eqs. (25) and (30) into Eq. (27), together with Eqs. (28) and (29), yields a closed-form equation for the pressure variation in scale L;

$$\frac{\partial P}{\partial t}=\frac{K}{2}\frac{\partial^2 P^2}{\partial z^2} \tag{31}$$

where the axial coordinates z^* and Z are transformed back to z and

$$K=R_e\epsilon^2/8\gamma M_0^2 \tag{32}$$

This equation is the same one that Ducoffe[4] derived on a rough assumption of local, steady, incompressible Poiseuille-flow within tubes. The present analysis lays a rigorous theoretical foundation for this equation.

The initial conditions in $P(t,z)$ are:

$$\left.\begin{aligned}&\text{Case A:}\quad P(0,0)=1\\&\qquad\quad P(0,z)=P_L(0);\ \text{given (for } 0<z\le 1)\\&\text{Case B:}\quad P(0,z)=1\quad(\text{for } 0\le z<1)\\&\qquad\quad P(0,1)=P_L(0);\ \text{given}\end{aligned}\right\} \tag{33}$$

and the boundary conditions for both of the cases are:

$$P(t,0)=1 \qquad \text{and} \qquad P(t,1)=P_L(t) \tag{34}$$

where $P_L(t)$ is a nondimensional cavity pressure.

IV. Cavity Pressure $\hat{P}_L(t)$

The dimension of the cavity of pressure transducers coupled with connectors to tubes is assumed to be small compared with the scale length L; and the local pressure difference within it, therefore, can be neglected as far as the pressure variation in scale L is concerned. The cavity pressure $\hat{P}_L$ is a function of time only. The gas within the cavity is subject to isothermal changes if the volume V is sufficiently small, but as V increases the effect of the heat transfer at cavity walls becomes smaller and the pressure variation within cavities can be regarded as adiabatic.

The equation of state for the ideal gas contained within the cavity is

$$\hat{P}_L V=Mk\hat{T}_L \tag{35}$$

where M and $\hat{T}_L$ are the mass and the temperature of the gas within cavities, respectively, and k is the gas constant. The increment of cavity pressure $\delta\hat{P}_L$, due to the gas leaking from the tube during a short time interval $\delta\hat{t}$, is

$$V\delta\hat{P}_L=k\hat{T}_L\delta M+Mk\delta\hat{T}_L=(k/c_v)\delta\hat{E}_L \tag{36}$$

where c_v is the specific heat of the gas at constant volume and $\delta\hat{E}_L$ is the increment of the internal energy within the cavity. The latter can be written,[7] with the kinetic energy of the gas being neglected,

$$\delta\hat{E}_L=\hat{\rho}A\overline{\hat{w}}\,\hat{h}\,\delta\hat{t}-\delta\hat{Q} \tag{37}$$

where

$$\hat{h}=c_p\hat{T}=c_v\hat{T}+\hat{P}/\hat{\rho} \tag{38}$$

c_p is the specific heat at constant pressure, $\hat{T}$ the temperature of the gas leaking into the cavity, A the cross-sectional area of the tube, $\overline{\hat{w}}$ the mean velocity of the flow leaking from tubes, and $\delta\hat{Q}$ the heat energy transferred to the cavity wall during the interval $\delta\hat{t}$; i.e.,

$$\delta\hat{Q}=\begin{cases}0 & \text{for adiabatic cavity walls}\\ \hat{\rho}A\overline{\hat{w}}\delta\hat{t}(\hat{h}-c_v\hat{T}_L) & \text{for constant temperature cavity walls}\end{cases} \tag{39}$$

Now, Eqs. (37-39) are substituted into Eq. (36) and a limit of $\delta\hat{t}\to 0$ is taken. With the aid of Eq. (35) and $\hat{P}=\hat{\rho}k\hat{T}$,

$$\frac{1}{\hat{P}_L}\frac{d\hat{P}_L}{d\hat{t}}=\frac{fA}{V}\overline{\hat{w}} \tag{40}$$

is obtained, where

$$f=\begin{cases}\gamma\hat{P}/\hat{P}_L & \text{for adiabatic cavity walls}\\ \hat{\rho}V/M & \text{for constant temperature cavity walls}\end{cases} \tag{41}$$

At the junction of the tube and the cavity, the pressure $\hat{P}$ is equal to the cavity pressure $\hat{P}_L$ and, if the cavity wall temperature $\hat{T}_L$ is assumed to be equal to the tube wall temperature $\hat{T}_0$ (which is equal to the temperature $\hat{T}$ of the gas within tubes), Eq. (41) may be rewritten as:

$$f=\begin{cases}\gamma & \text{for adiabatic cavity walls}\\ 1 & \text{for constant temperature cavity walls}\end{cases} \tag{42}$$

since

$$M/V=\hat{\rho} \tag{43}$$

holds for the latter case. With this assumption of $\hat{T}_L=\hat{T}_0$, Eq. (40) is also valid for flows leaking out of cavities.

From Eq. (25) $\overline{\hat{w}}$ is formed, nondimensional quantities are used, and Eq. (40) becomes

$$\frac{1}{P_L}\frac{dP_L}{dt}=-mK\left(\frac{\partial P}{\partial z}\right)_{z=1} \tag{44}$$

where

$$m=\frac{f\pi R^2L}{V}=\frac{f\pi\epsilon^2}{V/L^3} \tag{45}$$

and m/f is the ratio of the inside volume of tubes to that of cavities. In a limit of isothermal change, Eq. (44) reduces to Ducoffe's boundary condition[4] which was derived on a simple assumption of mass continuity.

Now, a new nondimensional time T is introduced as:

$$T=Kt \tag{46}$$

and the basic equations (31) and (44) are rewritten:

$$\frac{\partial P}{\partial T}=0.5\frac{\partial^2 P^2}{\partial z^2} \tag{47}$$

and

$$\left(\frac{\partial P}{\partial T}\right)_{z=1}=-\frac{m}{2}\left(\frac{\partial P^2}{\partial z}\right)_{z=1} \tag{48}$$

where $(P(T,z))_{z=1}=P_L(T)$.

V. Finite-Difference Approximations

Equation (47) is a nonlinear parabolic partial-differential equation and is similar to the equation of one-dimensional heat flow with heat conductivity proportional to temperature. No explicit analytic solution of this equation is ever known and Ducoffe[4] solved it numerically through an explicit difference scheme known to be unstable except for very small time steps. In order to assure stability and get reliable results, an implicit difference scheme (the ninth formula in Table 8.I of Ref. 8) is applied; i.e., Eq. (47) can be approximated by

$$3\frac{P_j^{n+1}-P_j^n}{\Delta T}-\frac{P_j^n-P_j^{n-1}}{\Delta T}=\frac{(\delta^2 P^2)_j^{n+1}}{(\Delta z)^2} \tag{49}$$

where

$$(\delta^2 u)_j=u_{j+1}-2u_j+u_{j-1} \tag{50}$$

Δz and ΔT are increments of the variables z and T, respectively, and $\Delta z=1/J$, J being an integer. The approximations to $P(n\Delta T, j\Delta z)$ are denoted by P_j^n with $(n=0,1,2,\ldots)$ and $(j=0,1,2,\ldots,J)$. The nonlinear terms are substituted with

$$(P^2)_j^{n+1}\simeq(P^2)_j^n+2P_j^n(P_j^{n+1}-P_j^n) \tag{51}$$

Furthermore, Eq. (48) is approximated through the same scheme by

$$3\frac{P_J^{n+1}-P_J^n}{\Delta T}-\frac{P_J^n-P_J^{n-1}}{\Delta T}=-\frac{m\Delta(P^2)_J^{n+1}}{\Delta z} \tag{52}$$

where

$$\Delta(u)_J=(u_{J+1}-u_{J-1})/2 \tag{53}$$

The difference equations (49) and (52) make a system of algebraic equations for P_j^{n+1}, $(j=1,2,\ldots,J)$ with a tridiagonal coefficient matrix whose inversion is accomplished by any one of the well-known procedures.[8] Equations (47) and (48) are thus integrated from the appropriate initial conditions, Eq. (33), up to any desired time. The numerical solutions were calculated for several cases using a NEAC 3200 mini-computer with 100-400 meshes in z and ΔT being initially small ($\Delta T=0.0001$), and increasing after every 100 time steps. The results are presented with the experimental ones in Sec. VII.

VI. Experimental Procedure

The test apparatus comprised two stainless tubes (0.317 and 0.624 mm i.d., 1.5 mm o.d., and 1000 mm in length), a solenoid valve (ScanCo #WO-602-1P-24T Fluid Switch Wafer with a Ledex Solenoid Drive Model S5-24) and a pressure transducer with small inner cavity volume (404 mm^3) and frequency response up to 13.7 kHz (Druck PDCR32). Three connectors with different inner volumes (2952, 414, and 170 mm^3) were provided to attach the transducer to tubes and six different values of m/f were obtained among combinations of two tubes and three connectors.

The ends of stainless tubes were cut squarely to their axis and fixed flush with the inner wall of a large pressure reservoir (which was made of 3 in. diam steel tube and had a volume of about 8×10^5 mm^3) and served as the static pressure holes without any more fittings. This arrangement was different from that of Ducoffe,[4] who used the orifices smaller than the inside diameter of tubes. Small but finite inner volume (about 94.3 mm^3) of the solenoid valve and its connecting vinyl tubing was added to the cavity volume when it was necessary (case B).

The output of the pressure transducer was recorded on the vertical axis of an oscilloscope whose time axis was triggered by the voltage change of the solenoid motor drive current. The time history of pressure variations was recorded photographically.

The tests were conducted first by changing the reservoir pressure $\hat{P}_0$ ranging from 2 atm to vacuum and keeping the cavity initial pressure $\hat{P}_L(0)$ atmospheric, and next by changing $\hat{P}_L(0)$ and keeping $\hat{P}_0$ atmospheric.

VII. Results and Discussion

The examples of the calculated time history of pressure distributions along tubes are presented in Figs. 2a (case A) and 2b (case B) for the initial cavity pressure twice that of the reservoir pressure ($P_L(0)\equiv\hat{P}_L(0)/\hat{P}_0=2$, $m=1.0$) and in Figs. 3a (case A) and 3b (case B) for the initial cavity pressure vacuum ($P_L(0)\equiv\hat{P}_L(0)/\hat{P}_0=0$, $m=1.0$). These figures show that the necessary nondimensional time for $\hat{P}_L(T)$ to settle to $\hat{P}_0$ does not differ much for case A and for case B for the same value of the cavity volume ratio m. The dependence of settling times on m and $P_L(0)$ is presented in Figs. 4a (case A) and 4b (case B), whose abscissae are nondimensional settling time $T_{0.95}$ for $\hat{P}_L(T)$ to settle to $\hat{P}_0$ within 5% of its initial difference between $\hat{P}_0$; i.e.,

$$\hat{P}_L(T_{0.95})=\hat{P}_0+0.05(\hat{P}_L(0)-\hat{P}_0) \tag{54}$$

The settling time $T_{0.95}$ depends strongly on m (or m/f), and the dependence on the initial nondimensional cavity pressure $P_L(0)$ is relatively weak. The agreement between the theory and the experiment is mostly good, with the constant-temperature cavity wall assumption $f=1$, but as $\hat{P}_0$ becomes larger, the discrepancies increase – it takes a longer time to settle to the same accuracy. This probably results from the appearance of turbulence within tubes as the Reynolds number increases. The dimensional real time $\hat{t}$ which

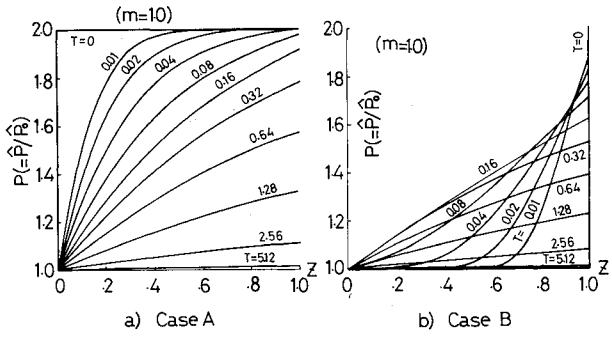

Fig. 2 Theoretical variation of pressures along tubes for $P_L(0)=2.0$ and $m=1.0$.

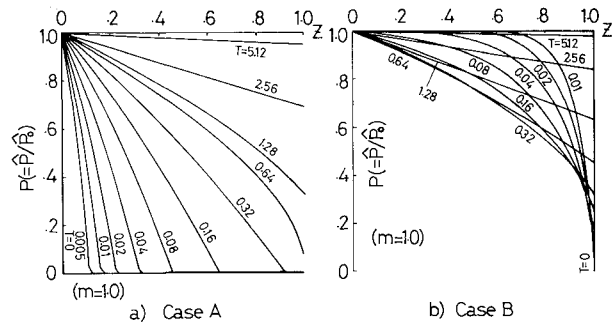

Fig. 3 Theoretical variation of pressures along tubes for $P_L(0)=0$ and $m=1.0$.

corresponds to T is, by definition,

$$\hat{t}=T(8\mu_0/\hat{P}_0)(L/R)^2 \tag{55}$$

and $\hat{t}$, for a fixed value of T, is shorter for larger $\hat{P}_0$ or for smaller R/L. These results show that Ducoffe's conclusion,[4] although he did not deal either with case B or $P_L(0)<1$ of case A, generally holds and can still be a good guide for pressure tubing design.

The time histories of the cavity pressure $P_L(T)$ are presented for several cases in Figs. 5a (case A, $m=0.137$) and 5b (case B, $m=0.118$). The agreement between the theory and the experiment is excellent for these particular examples, with the assumption of constant temperature cavity walls (i.e., $f=1$).

A theoretical propagation velocity of pressure disturbances within capillaries is finite for the present viscous flow theory, which can be predicted in analogy with the well-known equation of heat flow problems with thermal conductivities proportional to a positive power of temperature.[9] Any discontinuous pressure change will be smeared out by viscosity and no shock wavelike phenomena can be observed. Still, a front of sharp pressure rise propagates along tubes (Fig. 3a), and the initial state is kept essentially unchanged until this front passes. The propagation of the front is calculated for case A and presented in Fig. 6. The front is defined in this figure by the nondimensional pressure changes ΔP of 0.0001 and 0.01 from the initial constant state. Two different definitions give almost identical results for the compression front because of its sharp pressure rise, but for expansion, the front pressure rise is mild and the front locations are appreciably different for two definitions. In contrast to the inviscid one-dimensional flow theory, which says that the shock wave traveling into constant states is faster than the expansion wave, the velocity of the compression front is lower than that of the expansion one, and the velocity decreases as the local pressure gradient becomes small. Moreover, the velocity is independent of cavity volume ratios m, except very close to the cavity where the reflection from the open-end affects the front propagation. The dotted line for the expansion front in Fig. 6 is the limiting case of no end effect.

Once the solenoid valve is released, the front starts from the valve and travels to the other end of the system. Before this reaches the cavity, the cavity pressure $\hat{P}_L$ remains unchanged. A special connector with small cavity volume (the total cavity volume of 320 mm^3) was made and the lag time was measured. The nondimensional lag times are presented in Fig. 7. A theoretical lag time $T_{0.001}$ is defined as the period of the nondimensional pressure change ΔP of 0.001 from initial states. The theoretical lines T_{sonic} and T^*_{sonic} are defined under the assumption of the front traveling at sonic speeds, which is the conventional conclusion obtained from linear theories of transient fluid line responses.[10] For the case of $\hat{P}_0$ atmospheric

$$T_{\text{sonic}}=(\hat{P}_0/8\mu_0)(R/L)^2(L/a_0)=\text{const} \tag{56}$$

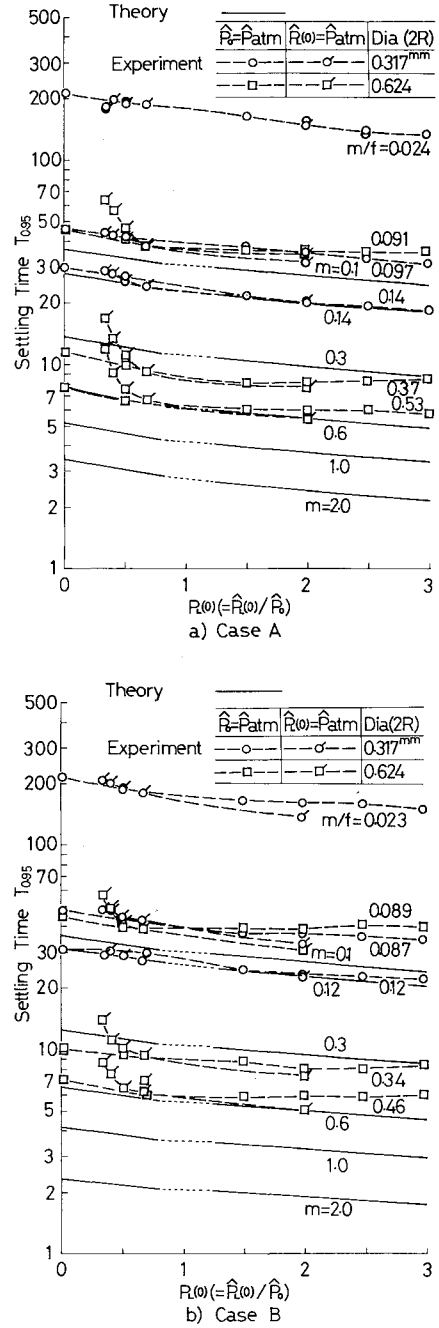

Fig. 4 Theoretical and experimental cavity pressure settling times $T_{0.95}$.

where the speed of sound a_0 is 347.2 m/s. For another case of varying $\hat{P}_0$, with the initial pressure atmospheric,

$$T^*_{\text{sonic}}=(\hat{P}_{\text{atm}}/8\mu_0)(R/L)^2(L/a_0)/P_L(0) \tag{57}$$

where $\hat{P}_{\text{atm}}$ is the atmospheric pressure and the curves T_{sonic} and T^*_{sonic} cross at $P_L(0)=1$. The experimental points come close to the line $T_{0.001}$ and tend to fall on the lines T_{sonic} or T^*_{sonic} as the Reynolds and Mach number increase. Supersonic velocities can scarcely be observed. The appearance of sonic front velocities invalidates the assumption of low subsonic flow within tubes, but the pressure difference as well as the flow velocity within tubes decreases rapidly once the front passes; therefore, the sonic front does not always limit the applicability of the predicted settling times.

A probable explanation of the physical mechanism of faster expansion fronts and slower compression ones is that the vorticity induced by the flow diffuses instantaneously into

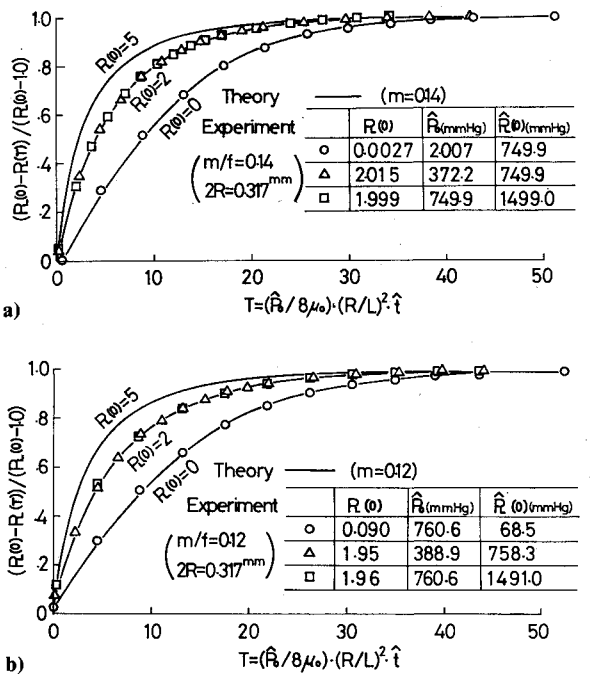

Fig. 5 Comparison of theoretical and experimental cavity pressure time variations: a) case A ($m = 0.14$); b) case B ($m = 0.12$).

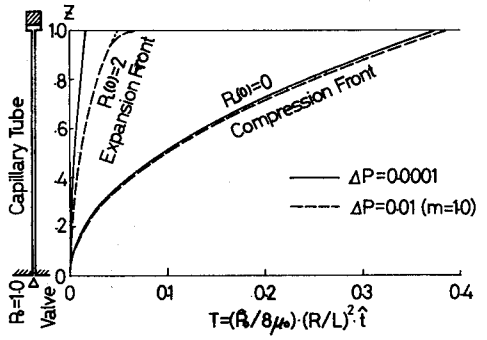

Fig. 6 Theoretical pressure-variation-front propagation histories.

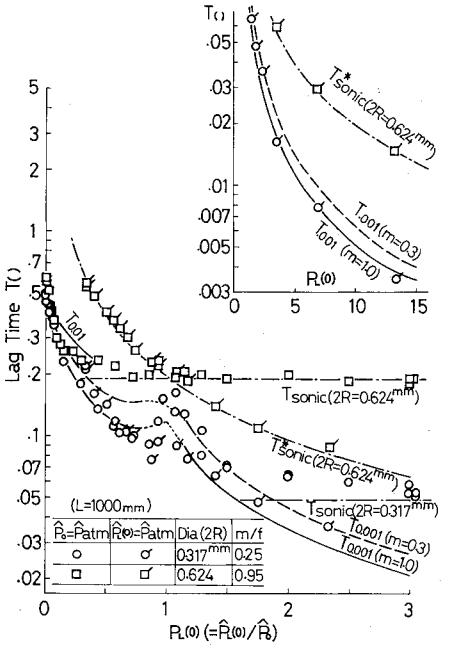

Fig. 7 Comparison of theoretical and experimental nondimensional lag times.

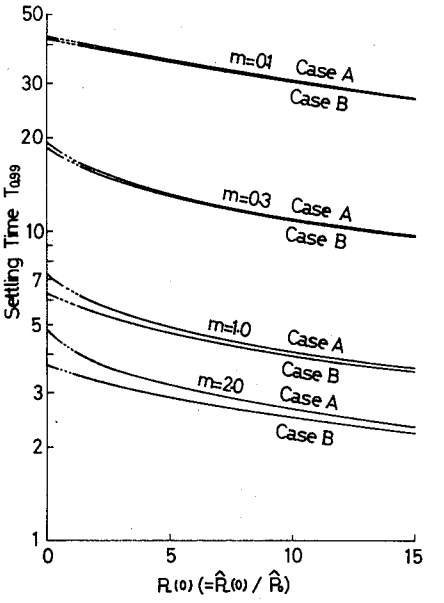

Fig. 8 Theoretical cavity pressure settling time $T_{0.99}$ vs initial to final pressure ratio $P_L(0)$.

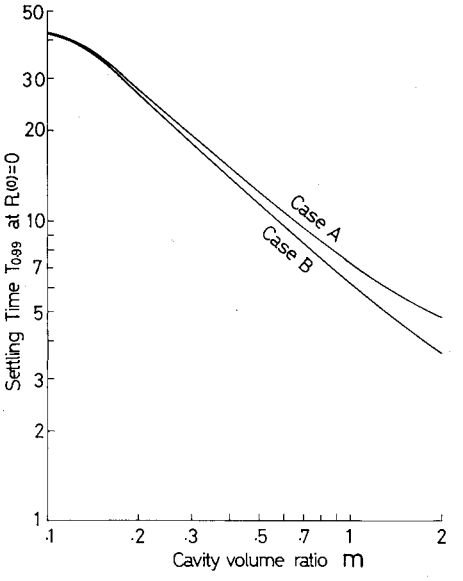

Fig. 9 Theoretical cavity pressure settling time $T_{0.99}$ at $P_L(0) = 0$ vs cavity volume ratio m.

tubes and this vorticity in turn induces flow which tends to decrease the local static pressure around the downstream end of fronts. This lower pressure decreases the pressure difference across the compression front and the velocity of the front is decreased, whereas for the expansion one the lower pressure increases the pressure difference across the front and increases its speed.

A quick estimation of the settling time $T_{0.99}$ (which is the time to settle $P_L(T)$ to 99% of its final value) is provided by assuming

$$\log_{10} T_{0.99} = aP_L(0) + \log_{10} b(m) \tag{58}$$

where a is obtained from the theoretical curves in Fig. 8 approximately as

$$\left.\begin{aligned} a &= -0.020 \quad \text{for case } A \\ a &= -0.013 \quad \text{for case B} \end{aligned}\right\} \tag{59}$$

and $b(m)$ is approximated by

$$\log_{10} b(m) = c \log_{10} m + d \tag{60}$$

where, from Fig. 9,

$$\left.\begin{aligned} c &= -0.78, \quad d = \log_{10} 7.5 \quad \text{for case A} \\ c &= -0.88, \quad d = \log_{10} 6.5 \quad \text{for case B} \end{aligned}\right\} \tag{61}$$

From Eqs. (58-61), the estimation formulas are

$$\left.\begin{aligned} T_{0.99} &= 10^{-0.02 P_L(0)} \times 7.5/m^{0.78} \quad \text{for case A} \\ T_{0.99} &= 10^{-0.013 P_L(0)} \times 6.5/m^{0.88} \quad \text{for case B} \end{aligned}\right\} \tag{62}$$

These equations give the lower limits of settling times $T_{0.99}$ approximately for $0 \le P_L(0) \le 15$ and $0.1 \le m \le 2$.

VIII. Concluding Remarks

The settling time of pressure-measuring instrumentation depends strongly on the tube radius to length ratio, $\epsilon = R/L$, and on the ratio of tube inside volume to transducer cavity volume. This cavity volume ratio, m/f, should be kept as small as possible to realize quick measurements for any given system. The settling time, moreover, depends only weakly on the initial pressure difference across tubes. The higher the absolute value of the pressure which is to be measured, the quicker the pressure settles. These conclusions are in line with the limited analysis due to Ducoffe.[4]

The constant temperature wall assumptions, both for cavity walls and for capillaries, give fair agreement between the theory and the experiments.

A sharp front of pressure variations propagates within capillaries and the velocity of the front is faster for the expansion front than for the compression one.

The onset of turbulence in tubes increases the settling time considerably. Equations (62) give a quick estimation of settling times under the assumption of laminar subsonic flow within tubes and give a lower limit of settling times for flows through thin capillary tubes.

Acknowledgment

This research was financially supported by the Grant in Aid for Scientific Research of the Ministry of Education, Japan.

References

[1] Stollery, J.L. and Murthy, A.V., "An Intermittent High-Reynolds-Number Wind Tunnel," *Aeronautical Quarterly,* Vol. 28, Nov. 1977, pp. 259-264.

[2] Davis, W.T., "Lag in Pressure Systems at Extremely Low Pressures," NACA TN 4334, 1958.

[3] Larcombe, M.J. and Peto, J.W., "The Response Times of Typical Transducer-Tube Configurations for the Measurement of Pressures in High-Speed Wind Tunnels," Aeronautical Research Council, London, C.P. No. 913, July 1965.

[4] Ducoffe, A.L., "Pressure Response in Supersonic Wind-Tunnel Pressure Instrumentation," *Journal of Applied Physics,* Vol. 24, Nov. 1953, pp. 1343-1354.

[5] Cole, J.D., "Two-Variable Expansion Procedures," *Perturbation Methods in Applied Mathematics,* 1st Ed., Blaisdell Publishing Co., Mass., 1968, pp. 79-119.

[6] Whitham, G.B., "Solutions for Which the Convection Terms Vanish," *Laminar Boundary Layers,* Rosenhead, L. (ed.), 1st Ed., Oxford University Press, Oxford, U.K., 1966, p. 135.

[7] Ichimatsu, T., "Change of State of Perfect Gases," *Engineering Thermodynamics,* 23rd Ed., Shokabo, Tokyo, Japan, 1967, pp. 46-65 (in Japanese).

[8] Richtmyer, R.D. and Morton, K.W., "Diffusion and Heat Flow," *Difference Methods for Initial-Value Problems,* 2nd Ed., Interscience Publishing Co., New York, 1967, pp. 185-217.

[9] Landau, L.D. and Lifshitz, E.M., "Thermal Conduction in an Infinite Medium," *Fluid Mechanics,* 1st English Ed., Pergamon Press, Oxford, U.K., 1959, pp. 192-195.

[10] Brown, F.T., "The Transient Response of Fluid Lines," *Transactions of the ASME,* Vol. 84, D, Dec. 1962, pp. 547-553.

Make Nominations for an AIAA Award

The following awards will be presented during the AIAA Aircraft Systems and Technology Meeting, August 4-6, 1980, Anaheim, Calif. If you wish to submit a nomination, please contact Roberta Shapiro, Director, Honors and Awards, AIAA, 1290 Avenue of the Americas, N.Y., N.Y. 10019 (212) 581-4300. The deadline date for submission of nominations is January 3, 1980.

Aircraft Design Award

"For the conception, definition or development of an original concept leading to a significant advancement in aircraft design or design technology."

General Aviation Award

"For outstanding recent technical excellence leading to improvements in safety, productivity or environmental acceptability of general aviation."

Haley Space Flight Award

"For outstanding contribution by an astronaut or flight test personnel to the advancement of the art, science or technology of astronautics, named in honor of Andrew G. Haley."

Support Systems Award

"For significant contribution to the overall effectiveness of aerospace systems through the development of improved support systems technology."